FEBS Letters 525 (2002) 156–163 FEBS 26355

Coupled rotation within single F_0F_1 enzyme complexes during ATP synthesis or hydrolysis

Georg Kaim[a,1], Michael Prummer[b,1], Beate Sick[b,1], Gert Zumofen[b], Alois Renn[b], Urs P. Wild[b], Peter Dimroth[a,*]

[a] *Institute of Microbiology, ETH Zürich, Schmelzbergstrasse 7, CH-8092 Zürich, Switzerland*
[b] *Physical Chemistry Laboratory, ETH Zürich, Wolfgang Pauli Strasse 10, CH-8093 Zürich, Switzerland*

Received 10 July 2002; accepted 13 July 2002

First published online 25 July 2002

Edited by Giorgio Semenza

Abstract **F_0F_1 ATP synthases are the smallest rotary motors in nature and work as ATP factories in bacteria, plants and animals. Here we report on the first observation of intersubunit rotation in fully coupled single F_0F_1 molecules during ATP synthesis or hydrolysis. We investigate the Na^+-translocating ATP synthase of *Propionigenium modestum* specifically labeled by a single fluorophore at one c subunit using polarization-resolved confocal microscopy. Rotation during ATP synthesis was observed with the immobilized enzyme reconstituted into proteoliposomes after applying a diffusion potential, but not with a Na^+ concentration gradient alone. During ATP hydrolysis, stepwise rotation of the labeled c subunit was found in the presence of 2 mM NaCl, but not without the addition of Na^+ ions. Moreover, upon the incubation with the F_0-specific inhibitor dicyclohexylcarbodiimide the rotation was severely inhibited.**

Key words: F_0F_1 ATP synthase; Single molecule; Intersubunit rotation; *Propionigenium modestum*

1. Introduction

F_0F_1 ATP synthases couple H^+ or Na^+ transport to the synthesis of ATP from ADP and phosphate using the energy of a transmembrane electrochemical gradient. The multisubunit enzyme complex comprises the membrane-extrinsic F_1 domain and the membrane-intrinsic F_0 domain (Fig. 1A). F_1 consists of five different subunits in an $\alpha_3\beta_3\gamma\delta\varepsilon$ stoichiometry. The F_0 moiety of bacteria is built from three different subunits in an ab_2c_n stoichiometry. Remarkably, the number of c subunits per F_0 subcomplex varies between species, i.e. 10 in yeast mitochondria [1], 11 in the bacterium *Ilyobacter tartaricus* [2], and 14 in spinach chloroplasts [3].

An exceptional reaction mechanism for the synthesis of ATP, first outlined on the basis of kinetic measurements [4], gained dramatic support by the X-ray structure of F_1 [5]. The new concept, designated the 'binding change mechanism', involves the intimate coupling of catalysis at F_1 and ion flux across F_0 by rotation of the rotor ($\gamma\varepsilon c_n$) against the stator ($ab_2\alpha_3\beta_3\delta$) (Fig. 1A). In order to achieve ATP synthesis, the transmembrane ion flow generates torque within F_0 that is transmitted by rotation of the rotor against the stator into conformational changes of the catalytic β subunits. Conversely, ATP hydrolysis would generate torque in F_1 that turns the rotor in the opposite direction and causes ion pumping.

During ATP hydrolysis, rotation of the γ subunit within the F_1 subcomplex has indeed been confirmed by biochemical [6–9] and spectroscopic techniques [10,11]. Most convincingly, the rotation of a micrometer-sized fluorescent actin filament attached to subunit γ has been directly visualized by video microscopy of single F_1 molecules [12] and rotation of γ could also be detected by single-fluorophore imaging [13]. It has been demonstrated that the ε subunit rotates together with γ [14,15] and that γ rotation proceeds in three discrete 120° steps [16]. Recently this approach has also been extended to the c subunit [17,18]. High-speed imaging revealed that a single 120° step is composed of two substeps of 90° and 30°, corresponding to ATP binding and ADP release, respectively [19]. One ATP was hydrolyzed per 120° motion and the torque of about 40 pN nm remains constant during rotation over a broad range of speed, load and ATP concentration [19].

Here, we use polarization-resolved confocal microscopy to study the rotation within the entire, functionally coupled F_0F_1 enzyme. Our study object is the Na^+-translocating ATP synthase from *Propionigenium modestum* and we investigate the Na^+ dependence of the rotation during ATP hydrolysis. Interestingly, this rotation could be blocked by the F_0-specific inhibitor *N,N′*-dicyclohexylcarbodiimide (DCCD). More important, by labeling of one c subunit with a single fluorophore and incorporation of F_0F_1 into liposomes, rotation during ATP synthesis could be observed. Rotation is initiated by the establishment of an electro-chemical Na^+ gradient across the liposome membrane, thus demonstrating the structural integrity of the F_0F_1 enzyme complex. These findings prove the tight chemo-mechanical coupling between the F_0 and the F_1 subcomplex.

2. Materials and methods

2.1. Synthesis of the F_0 subunits a, b and c from P. modestum in Escherichia coli and purification of the proteins

As described previously [20], *E. coli* PEF42 (DE3) containing plasmids pPmaHisN or pPmbHisC were used for the synthesis of subunits

*Corresponding author. Fax: (41)-1-632 13 78.
E-mail address: dimroth@micro.biol.ethz.ch (P. Dimroth).

[1] These authors contributed equally to this work.

Abbreviations: DCCD, *N,N′*-dicyclohexylcarbodiimide; NTA, nitrilotriacetic acid; ACF, autocorrelation function

0014-5793/02/$22.00
PII: S0014-5793(02)03097-1

a or b of the *P. modestum* ATP synthase, respectively. The recombinant a subunit contains an N-terminal fusion of 10 histidine residues and six histidines are genetically engineered to the C-terminal end of subunit b. After expression and solubilization from the membranes, both subunits were purified by Ni^{2+} affinity chromatography. The *P. modestum* subunit c was overexpressed and purified as described [21].

2.2. Mutagenesis and labeling of P. modestum subunit c

To obtain fluorophore-conjugated *P. modestum* subunit c, the Asp at position 2 was replaced by a Cys using the 'QuikChange' site-directed mutagenesis kit (Stratagene, La Jolla, CA, USA). Positive mutants were confirmed by DNA sequencing of both strands. The cyanine dye Cy3 was used as a label and Cy3-maleimide was produced from Cy3-NHS (Amersham Biosciences, Freiburg, Germany) as described [22]. Following established procedures [13], the genetically introduced single Cys residue was labeled with Cy3-maleimide at a labeling ratio of 0.93 mol Cy3 per mol c subunit.

2.3. Reconstitution of functional F_0F_1 complexes

A functional F_0 sector was reconstituted into liposomes from the purified a, b and c subunits of the Na^+-translocating ATP synthase of *P. modestum* [20]. During the reconstitution, the Cy3-labeled mutant c subunits were mixed with unlabeled wildtype c subunits at 1/15 to 1/25 ratios to minimize the occurrence of more than one fluorophore per F_0F_1. Under these conditions, the probability of one incorporated fluorophore is five times higher than the incorporation of two fluorophores. Singly labeled enzymes could be distinguished from doubly labeled complexes by detecting one bleaching event of Cy3 instead of two. Only data derived from singly labeled enzymes were used for further analysis.

Since the dye-labeled c subunit was separately modified, unspecific labeling of other F_0F_1 subunits can be excluded. After incubation of the F_0 liposomes with purified F_1 containing subunits α, β (with a N-terminal His_{10} tag), γ and ε from *E. coli* and subunit δ from *P. modestum* [20] and removal of residual F_1 by washing and centrifugation, the F_0F_1 holoenzyme was formed [20]. F_0F_1 complexes were solubilized by treatment with 0.5–1% Triton X-100, purified by Ni^{2+}-nitrilotriacetic acid (NTA) affinity chromatography and concentrated by precipitation with 12% polyethyleneglycol 6000. The pellet was dissolved in PGM buffer (5 mM potassium phosphate buffer, pH 7.5, 0.2 mM $MgCl_2$, 10% glycerol and 0.1% 2-mercaptoethanol) containing 0.05% Triton X-100 or K^+-cholate typically yielding an F_0F_1 concentration of 2 μM. The modification of single c subunits was found to be without effect on the Na^+-dependent ATP hydrolysis activity in comparison to the non-modified enzyme.

2.4. Reconstitution of in vitro assembled F_0F_1 into liposomes

Liposomes were generated by extruding a suspension in P buffer (5 mM potassium phosphate buffer, pH 7.5 with 0.2 mM $MgCl_2$) containing 2 mM NaCl through a 100 nm membrane for several minutes. A protein to lipid ratio of 1/400 ensured that there is on average one F_0F_1 complex per liposome. Thus, 25 μl (25 μg) of preformed F_0F_1 was reconstituted into 475 μl extruded liposomes (10 mg lipids). Within these proteoliposomes, we have rarely observed more than one Cy3 bleaching event indicating that the majority of the liposomes contained one F_0F_1 complex.

2.5. Ni-NTA coating of cover glasses

The glass surface of cover glasses (24×24 mm, Menzel, Braunschweig, Germany) was coated with Ni-NTA according to established protocols [13] with some modifications. After pre-cleaning by baking at 500°C for 2 h, the cover glasses were incubated in sealing solution (2% (v/v) 3-glycidylopropyl-trimethoxysilane (Fluka, Buchs, Switzerland), 0.01% (v/v) acetic acid) at 90°C for 3 h, coating solution (2% (w/v) *N*,*N*-bis(carboxymethyl)-L-lysine (Fluka, Buchs, Switzerland), 2 mM $KHCO_3$, pH 10.0) at 60°C for 16 h and Ni^{2+} solution (10 mM $NiSO_4$, 5 mM glycine, pH 8.0) at room temperature for at least 2 h. After each coating step, the cover glasses were rinsed with ultrapure water.

2.6. Immobilization of solubilized F_0F_1 and F_0F_1-containing liposomes

For immobilization, solubilized, in vitro assembled F_0F_1 was diluted 10^5-fold in PGM buffer and 10 μl of the dilution was dropped on an Ni-NTA-coated cover glass. Experiments under ATP hydrolysis conditions were performed in a total flow chamber volume of 50 μl PGM buffer equipped with an oxygen scavenging system consisting of 30 mM glucose, 0.3 mg/ml catalase and 0.2 mg/ml glucose oxidase and an ATP regenerating system consisting of 2.5 mM creatine phosphate and 0.2 mg/ml creatine kinase. The reaction was started with ATP concentrations of 0.5 μM or 2.5 mM. To examine the effect of Na^+ on rotation, the Na^+ concentration was increased from 50 μM to 1.5 mM. Inhibition experiments were conducted by incubating 20 μl of in vitro assembled F_0F_1 with 20 μM DCCD at low (< 50 μM) Na^+ concentrations for 15 min.

To immobilize F_0F_1-containing liposomes, the proteoliposome suspension was diluted 100-fold into P buffer. As a control, 40 μl of P buffer containing 2.5 mM ADP was dropped onto a bare cover glass and an image was taken as blank control. This contained less than three spots per 100 μm^2. Then, 5 μl of diluted proteoliposome suspension was added and immobilized by binding the His_{10}-tagged F_0F_1 to the Ni^{2+}-coated support. Upon inspection, well distributed fluorescence spots could be observed. To initiate ATP synthesis, a K^+/valinomycin diffusion potential of about 95 mV was established by adding 200 mM KCl and 2 nM valinomycin. Under our conditions a Na^+ concentration gradient of about 60 mV was additionally applied. In order to specifically inhibit the F_0 sector, the rotational behavior of single F_0F_1 molecules in reconstituted proteoliposomes was studied after incubation with 20 μM DCCD for 15 min.

2.7. Polarization-resolved confocal microscopy

The measurements were performed using a home-built scanning confocal fluorescence microscope [23]. A pulsed frequency-doubled Nd:YAG laser (Antares, Coherent) was focused onto the sample by an objective lens (Planapo 60×, NA 1.4, Nikon) to excite the fluorophores with circularly polarized light. The fluorescence emission was divided into the horizontal (I_V) and the vertical polarization component (I_H) and detected separately by two avalanche photo diodes (APDs, SPQ 141, Perkin Elmer). By computing the polarization $P(t) = (I_H - I_V)/(I_H + I_V) = \cos 2\phi(t)$ at discrete time intervals, the angle ϕ of the plane projection of the emission dipole moment of the fluorophore with respect to the horizontal axis can be determined. Analysis of $P(t)$, which is independent of the emission intensity, is advantageous, since I_H and I_V still depend on the out-of-plane orientation of the fluorophore.

2.8. Auto-correlation analysis.

The normalized polarization autocorrelation function (ACF) is defined as $\mathrm{ACF}(t) = \langle P(t'+t)P(t')\rangle / \langle P^2(t')\rangle$, where $P(t)$ is corrected for a linear drift and $\langle\ldots\rangle$ denotes time-averaging. By averaging over a longer observation time the signal-to-noise ratio is increased significantly leading to an enhanced time resolution. Hence, the use of autocorrelation techniques enables the analysis of fast rotational stepping as occurring in our experiments. The polarization ACF is closely related to the conditional probability $p(t,j|i)$ that the rotor is at the angular position Φ_i at time t when it was at the angular position Φ_j at time zero. The probabilities $p(t,j|i)$ are calculated by solving the Master equation $\dot{p} = Wp$, where W is made up from the rotational stepping rates. For the three-double-step model assuming only forward steps with rates k_1 and k_2 for the 90° and the 30° step, respectively, the solution of the ACF reads:

$$\mathrm{ACF}(t) = e^{-(k_1+k_2)/2}/2\mathrm{Re}\{(1+a)e^{\Omega t/2} + (1-a)e^{-\Omega t/2}\}$$

with

$$\Omega = \sqrt{(k_1-k_2)^2 - 2k_1k_2(1-i\sqrt{3})},$$

$$a = \{(k_1-k_2)^2 - 2k_1k_2(1-i\sqrt{3})\}/\{\Omega(k_1+k_2)\}$$

3. Results and discussion

To observe ATP-driven rotation of the c ring in a functionally coupled Na^+-translocating F_0F_1 ATP synthase, the holoenzyme was assembled from the individual a, b and c subunits of *P. modestum* and a hybrid F_1 complex containing subunit δ from *P. modestum* and the remaining subunits including a His_{10} tag-containing β subunit from *E. coli* [20]. Subunit c carrying a D2C substitution was labeled with the fluorophore

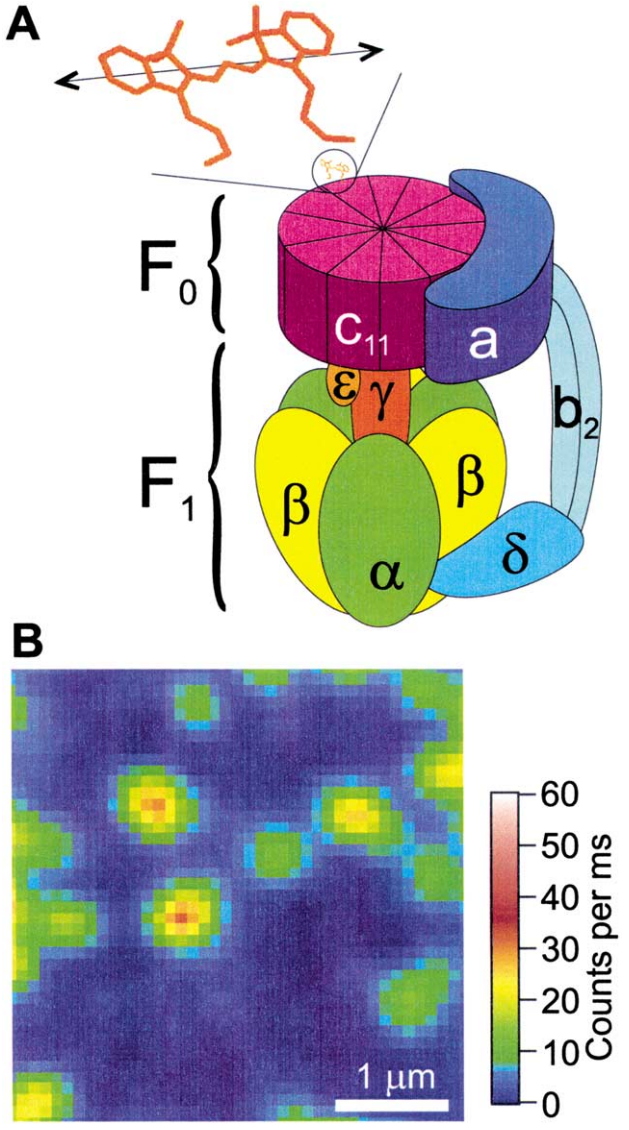

Fig. 1. Subunit composition and confocal microscopy of individual F_0F_1 holoenzymes. A: Subunit composition of F_0F_1 with a Cy3 fluorophore attached to one of the 11 c subunits via a genetically engineered single cysteine at position 2. The circle approximately indicates the real size of the fluorophore. B: Typical image of single fluorescently labeled F_0F_1 holoenzymes immobilized on a Ni-NTA-functionalized glass surface.

Cy3-maleimide and added to a 15–25-fold molar excess of wildtype subunit c during reconstitution to favor the incorporation of a single fluorescent c subunit into the ATP synthase complex. Confocal images of single immobilized F_0F_1 molecules were taken using circularly polarized laser excitation (Fig. 1B). Subsequently, individual molecules were selected and upon continuous excitation the fluorescence intensity was recorded until photo-bleaching occurred.

To study rotation during ATP hydrolysis we observed individual F_0F_1 proteins immobilized via their His tags on NTA-functionalized coverslips and covered with buffer (Fig. 2A). The constant polarization shown in Fig. 2B indicates a stable steady-state orientation and low rotational mobility of the fluorophore as well as the protein complex, both important preconditions for the ability to detect the rotation of the c subunit. The two traces were recorded in buffer containing only contaminating Na^+ concentrations (50 μM) and 0.5 μM ATP. Upon addition of 2 mM NaCl, stepwise changes of the polarization occurred and three discrete polarization levels could be detected (Fig. 2C). The dwell times in the polarization levels varied from 0.1 to 0.5 s. We assign this behavior to a complete stepwise rotation of the c_{11} rotor part of the enzyme during ATP hydrolysis. The corresponding ATP hydrolysis rates ranged from 2 to 10 s^{-1}, consistent with previous studies on the F_1 part of *E. coli* with similar low ATP concentrations [13–15,24]. The observation that Na^+ ions are obligatory for rotation of the c subunits proves the tight chemo-mechanical coupling of the F_0 part and the F_1 part in our Na^+-translocating ATPase. These data are in accordance with crosslinking experiments performed with the ATP synthase of *E. coli*: after bridging the rotor subunits γ, ε and c, coupled H^+ translocation and ATP synthesis activities were retained [25]. Direct visualization of c subunit rotation with the aid of attached actin filaments was also reported for the *E. coli* enzyme [17,18]. However, the rotation was not sensitive to DCCD and persisted in the cD61N mutant, which is known to lack any H^+-coupled ATP synthesis or hydrolysis activity [26]. These enzyme specimens were concluded to be decoupled at its ion motive portion [26], which is consistent with the observation that at the detergent concentrations used in rotation experiments, coupled H^+ translocation no longer exists [27].

In our experiments, uncoupling was avoided by removing the detergent via extensive washing of the sample with 3×500 μl PGM buffer after immobilization to the cover glass. Under these conditions, 72% of the single molecules rotate in the presence of 0.5 μM ATP and 2 mM NaCl. However, upon modification with 20 μM DCCD only 33% of the molecules show significant fluctuations of the fluorescent dye indicating the specific inhibition of intersubunit rotation within coupled F_0F_1 ATPases.

At higher ATP concentrations (2.5 mM), discrete steps could no longer be resolved in detail (Fig. 3A–C, left column). For an improved time resolution, a shorter integration time was required which led to a decrease in the signal-to-noise ratio. Therefore, autocorrelation techniques were used for the analysis of fast rotational events. The ACFs derived from the polarization time series are depicted in the right column of Fig. 3, together with confidence intervals. They exhibit an exponential decay for short time lags and significant long-ranging oscillations with a periodicity of 10 ms (Fig. 3A) to 20 ms (Fig. 3C). The oscillations result from random stepping rotations, which are observed only for a relatively short time interval. They are more pronounced than expected for an ACF obtained during an infinite detection period (for a more detailed discussion see below). Rotational frequencies of 25–50 Hz correspond to ATP hydrolysis rates of 75–150 ATP s^{-1} for different F_0F_1 enzymes with almost zero load. These data are consistent with ATP hydrolysis rates measured with the same F_0F_1 ensembles (100–120 s^{-1}).

The yield of rotating single molecules observed during ATP hydrolysis can be summarized as follows. About 90% of all ATPases analyzed exhibited a constant polarization in the absence or presence of ATP if no Na^+ was added. From the selected molecules 72% rotated after the addition of 2 mM NaCl. This high yield as compared to other investigations (0.4–5% of rotating actin filaments) [17,18] could be explained by the much smaller size of the single dye label,

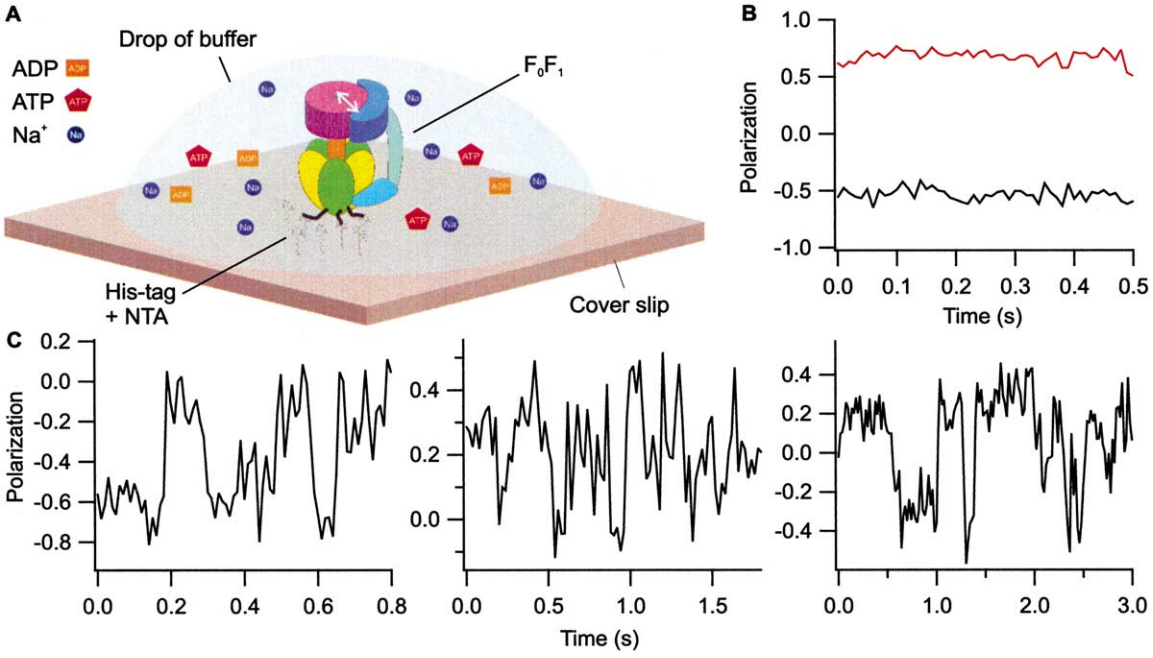

Fig. 2. Discrete rotational steps during ATP hydrolysis. A: Cy3-labeled enzymes were immobilized via their His tags on NTA-functionalized coverslips. B: Polarization signals of two different molecules recorded in the presence of 0.5 μM ATP in buffer with very low Na^+ concentration (50 μM). The constant polarization (+0.65 and −0.5) indicates a rigid attachment of the fluorophore to the well immobilized protein. The absence of rotation without Na^+ proves the tight chemo-mechanical coupling of the F_0 and the F_1 parts. C: Discrete changes of the polarization signal could be observed after the addition of 2 mM NaCl. This behavior can be interpreted as rotation during ATP hydrolysis, which is Na^+-dependent and therefore coupled.

and therefore the minimal sterical interference between the label and the F_0 part.

In vivo, the F_0F_1 holoenzyme is embedded in a phospholipid membrane and usually works in the ATP synthesis mode. To mimic physiological conditions and observe rotation during ATP synthesis, the Na^+-ATP synthase was incorporated in monodisperse liposomes (diameter 100 nm) and subsequently immobilized to Ni^{2+}-coated glass coverslips via the His_{10} tags on the β subunits (Fig. 4A). To start the ATP synthase activity, an electrochemical gradient has to be generated. In a first step, proteoliposomes loaded with 2 mM NaCl and potassium phosphate buffer were diluted into the same buffer containing in addition 2.5 mM ADP but no NaCl. At this stage, the electric potential is zero but a chemical Na^+ gradient equivalent to approximately 60 mV is present. Under these conditions a constant non-zero polarization was observed that exhibited no correlation (Fig. 4B), suggesting that the proteoliposomes were immobilized on the glass surface via the His tags of the protein and that rotation coupled to ATP synthesis did not occur. In ensemble measurements using the same proteoliposome preparation, no ATP synthesis could be detected even at Na^+ gradients of 120 mV and above. The addition of 200 mM KCl and 2 nM valinomycin triggers the electrogenic influx of potassium ions into the liposomes and establishes a diffusion potential of 95 mV. Under these conditions, large and fast fluctuations of the polarization signal were observed and the corresponding ACF exhibited periodic oscillations (Fig. 4C–E). These data indicate c ring rotation during ATP synthesis driven by a membrane potential but not by a Na^+ concentration gradient only. They are therefore in complete accord with our previous observation of an obligatory requirement of the electrical component of the driving force for ATP synthesis [28–30]. The ACFs of the three sequentially recorded polarization traces show oscillations with increasing period length probably due to the continuous consumption of the sodium motive force. The ACFs showed periodicities between 20 and 40 ms indicating rotational frequencies of 12.5–25 Hz (Fig. 4C–E). This is consistent with experimentally obtained values from identical F_0F_1 proteoliposomes indicating that ATP is indeed synthesized with rates of 45–60 ATP s^{-1} corresponding to rotational frequencies of 15–20 Hz. Furthermore, upon preincubation of the proteoliposomes with 20 μM DCCD, only small uncorrelated fluctuations were observed suggesting that rotation is again blocked by this F_0-specific inhibitor (Fig. 4F).

For a further interpretation of our observations we compared them to Monte Carlo simulations based on three different models suggested in the literature to describe the dynamics of this rotational motor. In the first single-molecule experiments on the F_1 part three steps per full rotation were observed [16]. More recently Yashuda and coworkers succeeded in resolving each of these three steps as a sequence of one 90° and one 30° step following nucleotide binding and release, respectively [19]. Furthermore, it has been proposed that the rotation of the holoenzyme during ATP synthesis should reveal 11 steps per revolution [31] because of the 11-fold symmetry of the rotor within the F_0 part of the enzyme [2].

Stepping rotation was simulated assuming an exponential distribution of dwell times in each step. The step width varies according to the model $(3\times2\pi/3,\ 3\times(\pi/2+\pi/6),\ 11\times2\pi/11)$. From the stepping rotation the polarization and then the ACF were computed. The number of simulated data points was comparable to the number of experimental data points per polarization time series. All models lead to an ACF with a decay at short time lags and long-ranging oscillations. With

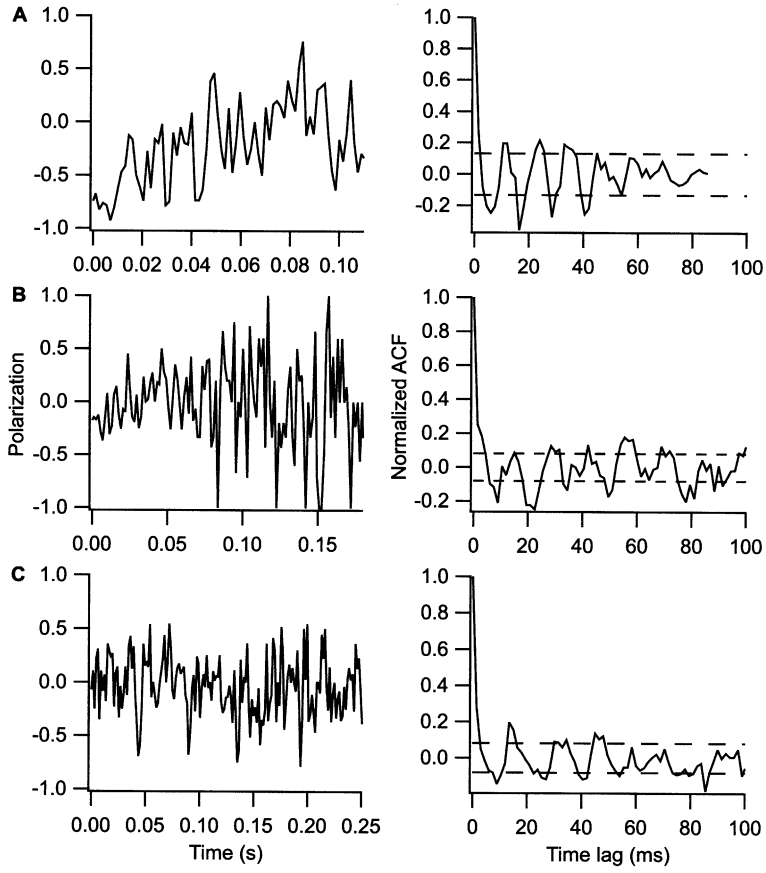

Fig. 3. Fast rotation of F_0F_1 in the hydrolysis mode with saturating ATP concentrations. A–C: Left column: Polarization traces of three different molecules. Individual steps cannot be resolved directly. Right column: Corresponding ACFs. Oscillations are observed when only a few revolutions are recorded due to periodic changes of the polarization.

increasing number of steps per revolution the ACF exhibits more pronounced and more regular oscillations. The variety within one model from run to run is significant (see two examples as dashed lines in Fig. 5A), similar as in the experimental data. By visual inspection it was found that the simulation based on the three-double-step model is most consistent with our data. This finding suggests that the ATP/ADP turnover is rate-limiting under Na^+ and nucleotide saturation conditions in both modes, ATP hydrolysis and synthesis.

The dynamics of a stochastic stepping rotor can also be described analytically using a Master equation approach [32]. The calculated ACF (Fig. 5A, solid line) comprises a modulated exponential decay, one pronounced minimum, and vanishing oscillatory contributions. The discrepancy between this analytic function and the simulations can be resolved by increasing the number of data points (Fig. 5A, dashed-dotted line). Moreover, also the experimental ACF eventually reproduces the analytic ACF when averaged over several individual molecules with similar stepping rates (Fig. 5B). Again, the three-double-step model fits slightly better to the data than the 11-step model. The reason for the appearance of more pronounced oscillations in the ACF of experimental and short simulated data sets is the limited number of observed revolutions. Therefore, from the expected bell-shaped distribution of rotation periods of a multi-step rotor [13] only a small subset of all possible periods is observed. With a high probability this undersampling leads to polarization traces that contain a narrow distribution of only a few frequencies (Fig. 5A, inset). Hence, the obtained ACFs comprise periodic correlations more long-ranging than the analytic solution would suggest.

In this single-fluorophore polarization study we have shown step-wise rotation of the rotor versus the stator in a functionally coupled Na^+-translocating F_0F_1 complex. The presence of sodium ions is an obligatory precondition for ATP hydrolysis [33] and thus rotation. Although the single-chromophore approach contains several experimental difficulties, e.g. low number of detected photons and ambiguity about the direction of rotation, it enabled us to detect rotation in single F_0F_1 molecules during ATP synthesis for the first time. Enzymes

→

Fig. 4. Observation of rotation during ATP synthesis. A: Cy3-labeled F_0F_1 was reconstituted into liposomes and immobilized on a glass surface. The proteoliposomes were filled with 2 mM NaCl and the surrounding buffer contained 2.5 mM ADP, 5 mM phosphate and 0.2 mM Mg^{2+}. B–F: Left column: polarization signals; right column: corresponding ACF. B: In the presence of a chemical Na^+ gradient of 60 mV, the polarization is constant, non-zero and non-correlated. C–E: After the addition of 200 mM KCl and 2 nM valinomycin a diffusion potential of 95 mV was applied, the sodium motive force induced ATP synthesis and rotation could be measured. F: When the proteoliposomes were pre-incubated with 20 μM DCCD, no rotation could be observed and the polarization fluctuations were uncorrelated.

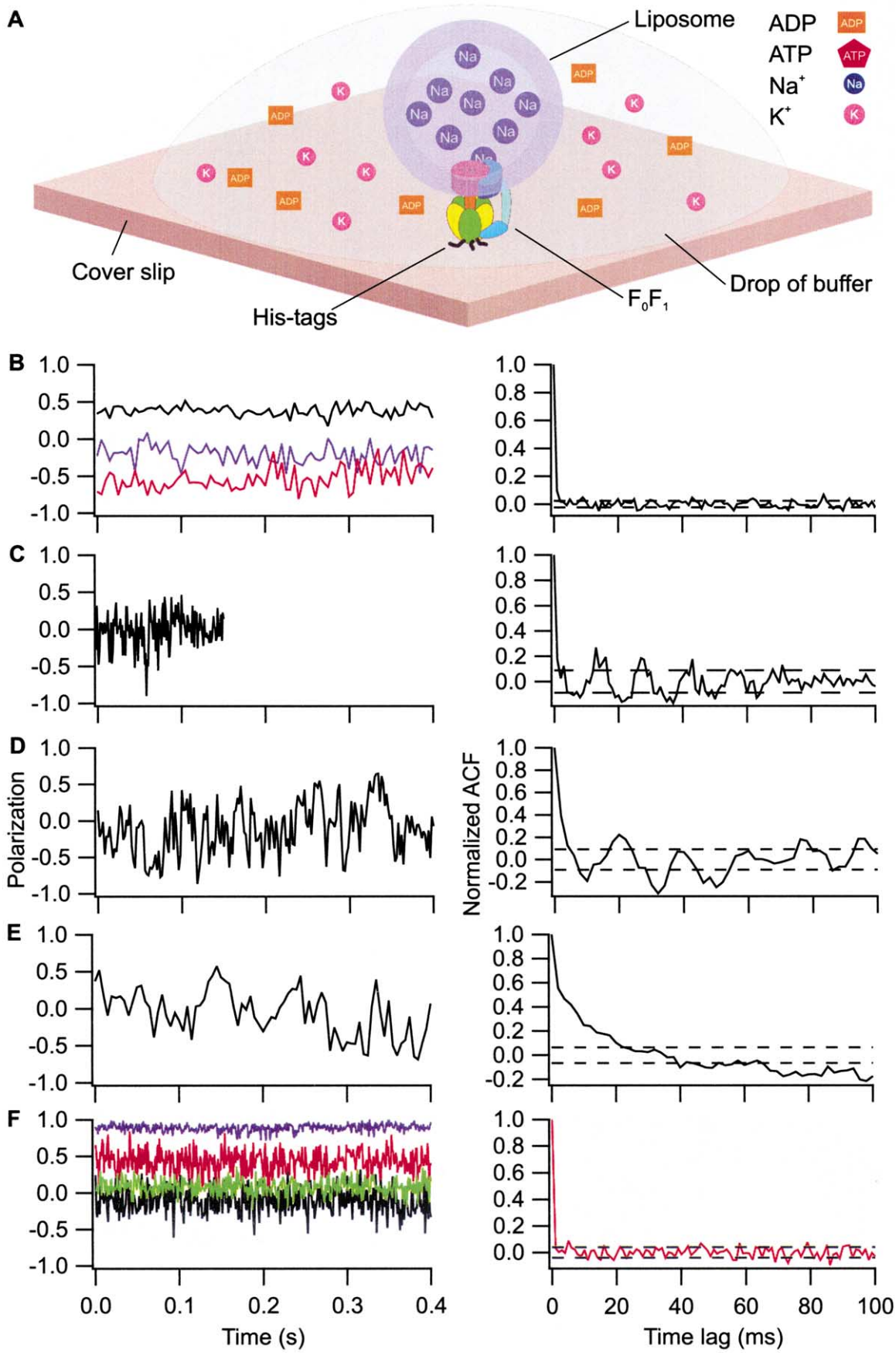
A
Liposome
ADP
ATP
Na+
K+
Cover slip
His-tags
F0F1
Drop of buffer
B
C
D
E
F
Polarization
Normalized ACF
Time (s)
Time lag (ms)

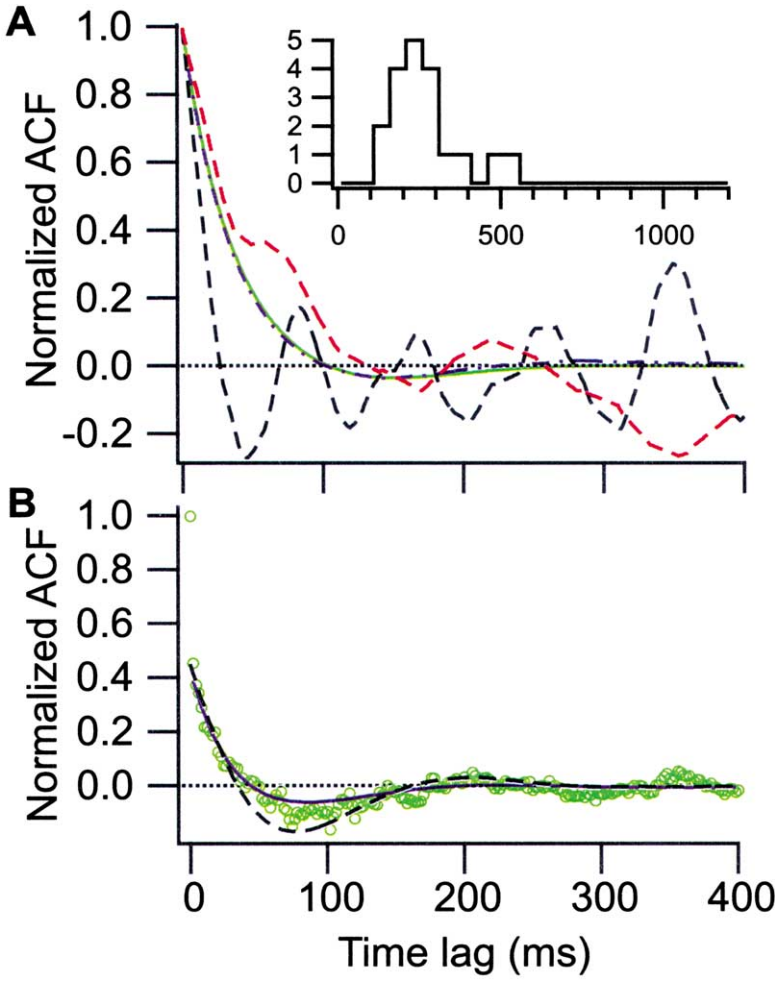

Fig. 5. Comparison of the ACFs from experiment, simulations, and theory. A: Two typical examples of simulations using 10^3 data points (red and black dashed line) resemble qualitatively the experimental data from short polarization traces. Inset: Histogram of rotation periods of the simulation leading to the dashed black ACF. In contrast, simulations with 10^6 data points (blue dashed dotted line) reproduce the analytic solution (green line). B: Averaged ACF of three molecules during ATP synthesis with similar decay time (green open circles). For comparison, the ACFs from the three-double-step model (blue solid line) and the 11-step model (black dashed line) are drawn.

incorporated in liposomes showed no rotation in the presence of a Na^+ concentration gradient only. However, after applying an electric potential difference, the rotor assembly turned with 12.5–25 Hz during ATP synthesis. This rotation was specifically inhibited by DCCD giving additional evidence that the enzyme used in this study was structurally and functionally the same as F_0F_1 complexes assembled in vivo.

References

[1] Stock, D., Leslie, A.G. and Walker, J.E. (2001) Science 286, 1700–1705.
[2] Stahlberg, H., Müller, D.J., Suda, K., Fotiadis, D., Engel, A., Meier, T., Matthey, U. and Dimroth, P. (2001) EMBO Rep. 2, 229–233.
[3] Seelert, H., Poetsch, A., Dencher, N.A., Engel, A., Stahlberg, H. and Müller, D.J. (2000) Nature 405, 418–419.
[4] Boyer, P.D. and Kohlbrenner, W.E. (1981) in: Energy Coupling in Photosynthesis (Selman, B. and Selman-Reiner, S., Eds.), pp. 231–240, Elsevier/North-Holland, New York.
[5] Abrahams, J.P., Leslie, A.G., Lutter, R. and Walker, J.E. (1994) Nature 370, 621–628.
[6] Duncan, T.M., Bulygin, V.V., Zhou, Y., Hutcheon, M.L. and Cross, R.L. (1995) Proc. Natl. Acad. Sci. USA 92, 10964–10968.
[7] Zhou, Y., Duncan, T.M., Bulygin, V.V., Hutcheon, M.L. and Cross, R.L. (1996) Biochim. Biophys. Acta 1275, 96–100.
[8] Zhou, Y., Duncan, T.M. and Cross, R.L. (1997) Proc. Natl. Acad. Sci. USA 94, 10583–10587.
[9] Aggeler, R., Ogilvie, I. and Capaldi, R.A. (1997) J. Biol. Chem. 272, 19621–19624.
[10] Sabbert, D., Engelbrecht, S. and Junge, W. (1996) Nature 381, 623–625.
[11] Sabbert, D., Engelbrecht, S. and Junge, W. (1997) Proc. Natl. Acad. Sci. USA 94, 4401–4405.
[12] Noji, H., Yasuda, R., Yoshida, M. and Kinosita Jr., K. (1997) Nature 386, 299–302.
[13] Adachi, K., Yasuda, R., Noji, H., Itoh, H., Harada, Y., Yoshida, M. and Kinosita Jr., K. (2000) Proc. Natl. Acad. Sci. USA 97, 7243–7247.
[14] Häsler, K., Engelbrecht, S. and Junge, W. (1998) FEBS Lett. 426, 301–304.
[15] Kato-Yamada, Y., Noji, H., Yasuda, R., Kinosita Jr., K. and Yoshida, M. (1998) J. Biol. Chem. 273, 19375–19377.
[16] Yasuda, R., Noji, H., Kinosita Jr., K. and Yoshida, M. (1998) Cell 93, 1117–1124.
[17] Sambongi, Y., Iko, Y., Tanabe, M., Omote, H., Iwamoto-Kihara, A., Ueda, I., Yanagida, T., Wada, Y. and Futai, M. (1999) Science 286, 1722–1724.
[18] Pänke, O., Gumbiowski, K., Junge, W. and Engelbrecht, S. (2000) FEBS Lett. 472, 34–38.

[19] Yasuda, R., Noji, H., Yoshida, M., Kinosita Jr., K. and Itoh, H. (2001) Nature 410, 898–904.
[20] Wehrle, F., Appoldt, Y., Kaim, G. and Dimroth, P. (2002) Eur. J. Biochem. 269, 2567–2573.
[21] Matthey, U., Kaim, G., Braun, D., Wüthrich, K. and Dimroth, P. (1998) Eur. J. Biochem. 261, 459–467.
[22] Tokunaga, M., Kitamura, K., Saito, K., Iwane, A.H. and Yanagida, T. (1997) Biochem. Biophys. Res. Commun. 235, 47–53.
[23] Prummer, M., Hubner, C.G., Sick, B., Hecht, B., Renn, A. and Wild, U.P. (2000) Anal. Chem. 72, 443–447.
[24] Kinosita Jr., K., Yasuda, R., Noji, H., Ishiwata, S. and Yoshida, M. (1998) Cell 93, 21–24.
[25] Tsunoda, S.P., Aggeler, R., Yoshida, M. and Capaldi, R.A. (2001) Proc. Natl. Acad. Sci. USA 98, 898–902.
[26] Junge, W., Pänke, O., Cherepanov, D.A., Gumbiowski, K., Müller, M. and Engelbrecht, S. (2001) FEBS Lett. 504, 152–160.
[27] Tsunoda, S., Aggeler, R., Noji, H., Kinosita Jr., K., Yoshida, M. and Capaldi, R. (2000) FEBS Lett. 470, 244–248.
[28] Kaim, G. and Dimroth, P. (1998) FEBS Lett. 434, 57–60.
[29] Kaim, G. and Dimroth, P. (1998) EMBO J. 17, 5887–5895.
[30] Kaim, G. and Dimroth, P. (1999) EMBO J. 18, 4118–4127.
[31] Dimroth, P., Wang, H., Grabe, M. and Oster, G. (1999) Proc. Natl. Acad. Sci. USA 96, 4924–4929.
[32] van Kampen, N.G. (1992) in: Stochastic Processes in Physics and Chemistry, 2nd edn., Elsevier/North-Holland, New York.
[33] Kluge, C. and Dimroth, P. (1993) J. Biol. Chem. 268, 14557–14560.